

# Azinium–(π-Bridge)–Pyrrole NLO-Phores: Influence of Heterocycle Acceptors on Chromophoric and Self-Assembled Thin-Film Properties<sup>#</sup>

Antonio Facchetti,<sup>\*,†</sup> Alessandro Abbotto,<sup>†</sup> Luca Beverina,<sup>†</sup>  
Milko E. van der Boom,<sup>‡</sup> Pulak Dutta,<sup>§,⊥</sup> Guennadi Evmenenko,<sup>§,⊥</sup>  
Tobin J. Marks,<sup>||,⊥</sup> and Giorgio A. Pagani<sup>\*,†</sup>

Department of Material Science, University of Milano-Bicocca, via Cozzi 53, 20125 Milano, Italy, Department of Organic Chemistry, The Weizmann Institute of Science, Rehovot, 76100, Israel, Department of Chemistry, Department of Physics and Astronomy, and Materials Research Center, Northwestern University, Evanston, Illinois 60208-3113

Received May 9, 2002. Revised Manuscript Received September 25, 2002

Novel heterocycle-based azine/azinium–(π-bridge)–pyrrole systems, [(1-(pyrid-4-yl)-2-(N-methylpyrrol-2-yl)]ethene (**1**), 5-[(N-methylpyrrol-2-yl)azo]quinoline (**2**), 5-[(N-methylpyrrol-2-yl)azo]isoquinoline (**3**), and the corresponding *N*-methotriflates **4–6** were synthesized and characterized. Chromophore precursors **1–3** react with iodobenzyl-functionalized surfaces (**10**) affording polar-ordered  $\sigma$ -bonded thin films **7–9**, respectively. All systems were studied by optical (UV–visible, photoluminescence) spectroscopies, electrochemical (CV), and thermal (TGA, DSC) techniques. Self-assembled chromophore monolayers **7–9** on glass, quartz, and silicon substrates have been characterized by a full complement of physicochemical techniques: optical spectroscopy, aqueous advancing contact angle measurements, specular X-ray reflectivity, atomic force microscopy, and angle-dependent polarized second harmonic generation. Film second harmonic generation responses  $\chi^{(2)}$  vary more than 1 order of magnitude ranging from 1.3 and 1.6, to  $34 \times 10^{-8}$  esu for **9**-, **8**-, and **7**-based monolayers, respectively. This study demonstrates the following: (i) SA monolayers can be prepared using various types of azine-containing precursors; (ii) chromophore and SA film properties are influenced predominantly by the nature of the π-deficient azinium acceptor; (iii) unsubstituted, π-excessive pyrrol-2-yl rings can act as *primary* donor groups in push–pull conjugated systems.

## Introduction

Intrinsically acentric, self-assembled (SA) organic films covalently bound to solid substrates have received much attention over the past decade.<sup>1,2</sup> These layer-by-layer systems are generally more robust than LB-type

films<sup>3</sup> and exhibit controlled, tunable physical and chemical properties.<sup>1,4</sup> Most attractive is the fabrication of covalently grafted photonic/electronically functionalized thin films since these materials can be integrated into “all-organic” light-processing devices (e.g., electrooptic modulators, frequency-doubling waveguides).<sup>5</sup> In particular, chemisorptive siloxane-based self-assembly is known to yield densely packed organic films on hydrophilic substrates.<sup>6–8</sup> Various assemblies containing porphyrin- and calixarene-based derivatives and rodlike alkynyl and stilbazolium dyes, exhibiting large electrooptic responses, have been prepared by this approach.<sup>9</sup> These chromophores are usually covalently

<sup>#</sup> This paper is dedicated to Professor Andrew Streitwieser, Jr. on the occasion of his 75th birthday.

\* Corresponding authors. E-mail: a-facchetti@northwestern.edu; giorgio.pagani@mater.unimib.it.

<sup>†</sup> University of Milano-Bicocca.

<sup>‡</sup> The Weizmann Institute of Science.

<sup>§</sup> Department of Physics and Astronomy, Northwestern University.

<sup>||</sup> Department of Chemistry, Northwestern University.

<sup>⊥</sup> Materials Research Center, Northwestern University.

(1) *New Developments in Construction and Function of Organic Thin Films*; Möbius D., Miller, R., Eds.; Elsevier: Amsterdam, 1996.

(2) (a) Van Cott, K. E.; Guzy, M.; Neyman, P.; Brands, C.; Heflin, J. R.; Gibson, H. W.; Davis, R. M. *Angew. Chem., Int. Ed. Engl.* **2002**, *17*, 3226–3228. (b) Bakamoh, S. B.; Blanchard, G. J. *Langmuir* **2001**, *17*, 3438–3446. (c) van der Boom, M. E.; Evmenenko, G.; Dutta, P.; Marks, T. J. *Adv. Funct. Mater.* **2001**, *11*, 393–397. (d) Neff, G. A.; Helfrich, M. R.; Clifton, M. C.; Page, C. J. *J. Chem. Mater.* **2000**, *12*, 2363–2371. (e) Flory, W. C.; Mehrens, S. M.; Blanchard, G. J. *J. Am. Chem. Soc.* **2000**, *122*, 7976–7985. (f) Doron-Mor, H.; Hatzor, A.; Vaskevich, A.; van der Boom-Moav, T.; Shanzer, A.; Rubinstein, I.; Cohen, H. A. *Nature* **2000**, *406*, 382–385. (g) Hanken, D. G.; Naujok, R. R.; Gray, J. M.; Corn, R. M. *Anal. Chem.* **1997**, *69*, 240–248. (h) Yitzchaik, S.; Marks, T. J. *Acc. Chem. Res.* **1996**, *29*, 197–202. (i) Marks, T. J.; Ratner, M. *Angew. Chem., Int. Ed. Engl.* **1995**, *34*, 155–173. (j) Katz, H. E.; Wilson, W. L.; Scheller, G. *J. Am. Chem. Soc.* **1994**, *116*, 6636–6640. (k) Katz, H. E.; Wilson, W. L.; Scheller, G. *J. Am. Chem. Soc.* **1994**, *116*, 6636–40.

(3) (a) Schwartz, H.; Mazor, R.; Khodorkovsky, V.; Shapiro, L.; Klug, J. T.; Kovalev, E.; Meshulam, G.; Berkovic, G.; Kotler, Z.; Efrima, S. *J. Phys. Chem. B* **2001**, *105*, 5914–5921. (b) Johal, M. S.; Parikh, A. N.; Lee, Y.; Casson, J. L.; Foster, L.; Swanson, B. L.; McBranch, D. W.; Li, D. Q.; Robinson, J. M. *Langmuir* **1999**, *15*, 1275–1282. (c) Roscoe, S. B.; Yitzchaik, S.; Kakkar, A.; Marks, T. J.; Xu, Z.; Zhang, T.; Lin, W.; Wong, G. K. *Langmuir* **1996**, *12*, 5338–5349. (d) Freeman, T. L.; Evans, S. D.; Ulman, A. *Langmuir* **1995**, *11*, 4411–4417. (e) Ulman, A. *Organic Thin Films and Surfaces: Directions for the Nineties*; Academic Press: New York, 1995. (f) Ulman, A. *An Introduction to Ultrathin Organic Films: From Langmuir–Blodgett to Self-Assembly*; Academic Press: New York, 1991.

(4) (a) Ulman, A.; Tillman, N. *Langmuir* **1989**, *5*, 1418–1420. (b) Lee, H.; Kepley, L. J.; Hong, H. G.; Mallouk, T. E. *J. Am. Chem. Soc.* **1988**, *110*, 618–620. (c) Allara, D. L.; Atre, S. V.; Elliger, C. A.; Snyder, R. G. *J. Am. Chem. Soc.* **1991**, *113*, 1852–1854. (d) Davis, W. B.; Svec, W. A.; Ratner, M. A.; Wasielewski, M. R. *Nature* **1998**, *396*, 60–63.

linked to substrate surface via  $N$ -alkyl- or  $N$ -benzylpyridinium rings.<sup>9,10</sup> However, SA polar films containing push-pull/donor-acceptor NLO-phores based on other  $\pi$ -deficient aza-heterocycle as acceptors and  $\pi$ -excessive heterocycles as donor are essentially unknown.<sup>11</sup>

The classic design of highly polarizable organic structures, with large intramolecular charge-transfer excitations, requires the conjugation of donor (D) and acceptor (A) groups through a  $\pi$ -backbone. The molecular polarization of such systems has key implications for optical

(5) (a) van der Boom, M. E. *Angew. Chem., Int. Ed. Engl.* **2002**, *18*, 3363–3366. (b) *Organic Thin Films for Waveguiding Nonlinear Optics*; Kajzar, F., Swalen, J. D., Eds.; Gordon and Breach Publishers: Langhorne, PA, 1996. (c) Zhao, Y.-G.; Wu, A.; Lu, H.-L.; Chang, S.; Lu, W.-K.; Ho, S.-T.; van der Boom, M. E.; Malinsky, J. E.; Marks, T. J. *Appl. Phys. Lett.* **2001**, *79*, 587–589. (d) Enami, Y.; Poyhonen, P.; Mathine, D. L.; Bashar, A.; Madasamy, P.; Honkanen, S.; Kippelen, B.; Peyghambarian, N.; Marder, S. R.; Jen, A. K.-Y.; Wu, J. *Appl. Phys. Lett.* **2000**, *76*, 1086–1088. (e) Lundquist, P. M.; Lin, W.; Zhou, H.; Hahn, D. N.; Yitzchaik, S.; Marks, T. J.; Wong, G. K. *Appl. Phys. Lett.* **1997**, *70*, 1941–1943. For recent studies of poled-polymer EO modulators, see: (f) Ma, H.; Chen, B.; Sassa, T.; Dalton, L. R.; Jen, A. K. *J. Am. Chem. Soc.* **2001**, *123*, 987–988. (g) Dalton, L. R.; Steier, W. H.; Robinson, B. H.; Zhang, C.; Ren, A.; Garner, S.; Chen, A. T.; Londergan, T.; Irwin, L.; Carlson, B.; Fifield, L.; Phelan, G.; Kincaid, C.; Amend, J.; Jen, A. *J. Mater. Chem.* **1999**, *9*, 1905–1920. For recent reviews and books, see: (h) Würthner, F.; Wortmann, R.; Meerholz, K. *ChemPhysChem* **2002**, *3*, 17–31. (i) Robinson, B. H.; Dalton, L. R.; Harper, A. W.; Ren, A.; Wang, F.; Zhang, C.; Todorova, G.; Lee, M.; Anisfeld, R.; Garner, S.; Chen, A.; Steier, W. H.; Houbrech, S.; Persoons, A.; Ledoux, I.; Zysy, J.; Jen, A. K. *Chem. Phys.* **1999**, *245*, 35–50. (j) Marder, S. R.; Kippelen, B.; Jen, A. K. Y.; Peyghambarian, N. *Nature* **1997**, *388*, 845–851. (k) Prasad, P. N.; Willam, D. J. *Introduction to Nonlinear Optical Effects in Molecules and Polymers*; Wiley: New York, 1991. For some recent examples on NLO compounds and materials, see: (l) Lemaître, N.; Attias, A. J.; Ledoux, I.; Zysy, J. *Chem. Mater.* **2001**, *13*, 1420–1427. (m) Würthner, F.; Yao, S.; Schilling, J.; Wortmann, R.; Redi-Abshire, M.; Mecher, E.; Gallego-Gomez, F.; Meerholz, K. *J. Am. Chem. Soc.* **2001**, *123*, 2810–2824. (n) Rekai, E. D.; Baudin, J.-B.; Jullien, L.; Ledoux, I.; Zysy, J.; Blanchard-Desce, M. *Chemistry* **2001**, *7*, 4395–4402. (o) Alheim, M.; Barzoukas, M.; Bedworth, P. V.; Blanchard-Desce, M.; Fort, A.; Hu, Z.-Y.; Marder, S. R.; Perry, J. W.; Runser, C.; Staehelin, M.; Zysset, B. *Science* **1996**, *271*, 335–337.

(6) (a) van der Boom, M. E.; Evmenenko, G.; Dutta, P.; Marks, T. J. *Langmuir* **2002**, *18*, 3704–3707. (b) van der Boom, M. E.; Evmenenko, G.; Dutta, P.; Marks, T. J. *Polym. Mater. Sci. Eng.* **2002**, *87*, 375–376. (c) Facchetti, A.; Abbott, A.; Beverina, L.; van der Boom, M. E.; Marks, T. J.; Pagani, G. A. *Polym. Prepr.* **2002**, *43*, 1292–1293. (d) van der Boom, M. E.; Richter, A. G.; Malinsky, J. E.; Dutta, P.; Marks, T. J. *Chem. Mater.* **2001**, *13*, 15–17. (e) van der Boom, M. E.; Richter, A. G.; Malinsky, J. E.; Dutta, P.; Marks, T. J.; Lee, P. A.; Armstrong, N. R. *Polym. Mater. Sci. Eng.* **2000**, *83*, 160–161. (f) van der Boom, M. E.; Richter, A. G.; Malinsky, J. E.; Dutta, P.; Marks, T. J. In *NSLS Activity Report; Science Highlights*; Corwin, M. A., Ehrlich, S. N., Eds.; Brookhaven Science Associates, Inc.: Upton, NY, 1999; Vol. 2, pp 47–49. (g) Li, D.-Q.; Ratner, M. A.; Marks, T. J. *J. Am. Chem. Soc.* **1990**, *112*, 7389–7390.

(7) (a) Hung, W.; Helvenston, M.; Casson, J. L.; Wang, R.; Bardeau, J.-F.; Lee, Y.; Johal, M. S.; Swanson, B. I.; Robinson, J. M.; Li, D.-Q. *Langmuir* **1999**, *15*, 6510–6514. (b) Li, D.-Q.; Swanson, B. I.; Robinson, J. M.; Hoffbauer, M. A. *J. Am. Chem. Soc.* **1993**, *115*, 6975–6980.

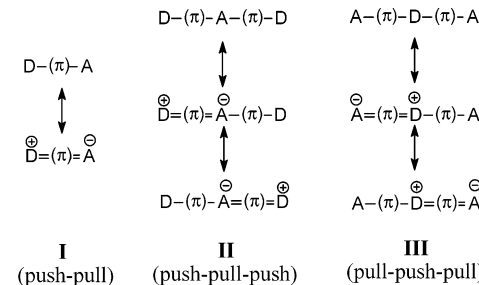
(8) (a) Moaz, R.; Sagiv, J. *Langmuir* **1987**, *3*, 1034–1044. (b) Moaz, R. Y. R.; Berkovic, G.; Sagiv, J. In *Thin Films*; Ulman, A., Ed.; Academic Press: San Diego, 1995; Vol. 4, pp 41–66. (c) Wasserman, S. R.; Tao, Y.-T.; Whitesides, G. M. *Langmuir* **1989**, *5*, 1074–1087. (d) Ulman, A. *Chem. Rev.* **1996**, *96*, 1533–1554. (e) van der Veen, N. J.; Flink, S.; Deij, M. A.; Egberink, R. J. M.; van Veggel, F. C. J. M.; Reinhoudt, D. N. *J. Am. Chem. Soc.* **2000**, *122*, 6112–6113.

(9) (a) Li, D. Q.; Swanson, B. I.; Robinson, J. M.; Hoffbauer, M. A. *J. Am. Chem. Soc.* **1993**, *115*, 6975. (b) Kakkar, A. K.; Yitzchaik, S.; Roscoe, S. B.; Marks, T. J.; Lin, W.; Wong, G. K. *Thin Solid Films* **1994**, *242*, 142. (c) Kakkar, A. K.; Yitzchaik, S.; Roscoe, S. B.; Kubota, F.; Allan, D. S.; Marks, T. J.; Lin, W.; Wong, G. K. *Langmuir* **1993**, *9*, 388. (d) Li, D. Q.; Ratner, M. A.; Marks, T. J. *J. Am. Chem. Soc.* **1990**, *112*, 7389. (e) Yang, X.; McBranch, D. W.; Swanson, B. I.; Li, D. Q. *Angew. Chem., Int. Ed. Engl.* **1996**, *35*, 538.

(10) Huang, W.; Helvenston, M.; Casson, J. L.; Wang, R.; Bardeau, J.-F.; Lee, Y.; Johal, M. S.; Swanson, B. I.; Robinson, J. M.; Li, D. *Langmuir* **1999**, *15*, 6510–6514.

(11) SA alkyl quinolinium salts have been described for tuning the electronic properties of silicon surfaces: Cohen, R.; Zenou, N.; Cahen, D.; Yitzchaik, S. *Chem. Phys. Lett.* **1997**, *279*, 270–274.

response at the molecular level.<sup>12</sup> Empirical recipes<sup>13</sup> assist chemists in properly selecting/combining D and A with A in order to enhance desired optical performance and properties. For instance, an active second-order NLO chromophore must have a noncentrosymmetric charge distribution (type **I**), whereas for third-order



NLO applications, symmetric structures (types **II** and **III**) are often more efficient systems. These  $\pi$ -conjugated structures may also be integrated into nanoscale assemblies (e.g., into molecular wires), where electrons can tunnel or hop through conjugated systems.<sup>14</sup>

In a recent series of papers,<sup>15,16</sup> several of us showed that the judicious combination of  $\pi$ -excessive (pyrrole, indole, thiophene) and  $\pi$ -deficient (pyridine, diazines, quinoline, isoquinoline) heterocycles<sup>17</sup> affords chromophores of type **I**–**III**, all valuable systems for both second- and third-order NLO processes. Zwitterionic dyes have been found to have potential for applications in photonic and electrooptic materials when incorporated into Langmuir–Blodgett<sup>18</sup> and acentric siloxane-based films.<sup>19</sup> In addition, we demonstrated that some pyridinium-based salts exhibit up-converted lasing and

(12) Shen, Y. R. *Principles of Nonlinear Optics*; Wiley: New York, 1984.

(13) For discussion of second-order NLO chromophores, see: (a) Lacroix, P. G. *Eur. J. Inorg. Chem.* **2001**, 339–348. (b) Bublitz, G. U.; Ortiz, R.; Runser, C.; Fort, A.; Barzoukas, M.; Marder, S. R.; Boxer, S. G. *J. Am. Chem. Soc.* **1997**, *119*, 2311–2312. (c) Marder, S. R.; Perry, J. W.; Bourhill, G.; Gorman, C. B.; Tiemann, B. G.; Mansour, K. *Science* **1993**, *261*, 186–189. For third-order NLO dyes, see: (d) Ventelon, L.; Moreaux, L.; Mertz, J.; Blanchard-Desce, M. *Chem. Commun.* **1999**, *20*, 2055–2056. (e) Albota, M.; Beljonne, D.; Bredas, J. L.; Ehrlich, J. E.; Fu, J. Y.; Heikal, A. A.; Hess, S. E.; Kogej, T.; Levin, M. D.; Marder, S. R.; McCordmaughon, D.; Perry, J. W.; Rockel, H.; Rumi, M.; Subramaniam, C.; Webb, W. W.; Wu, I. L.; Xu, C. *Science* **1998**, *281*, 1653–1656. (f) Reinhardt, B. A.; Brott, L. L.; Clarson, S. J.; Dillard, A. G.; Bhatt, J. C.; Kannan, R.; Yuan, L. X.; He, G. S.; Prasad, P. N. *Chem. Mater.* **1998**, *10*, 1863–1874.

(14) (a) Ratner, M. A.; Jortner, J. *Molecular Electronics*; Blackwell: Oxford, U.K., 1997. (b) Wasielewski, M. R. *Chem. Rev.* **1992**, *92*, 435. (c) Davis, W. B.; Ratner, M. A.; Wasielewski, M. R. *J. Am. Chem. Soc.* **2001**, *123*, 7877–7886.

(15) (a) Abbott, A.; Bradamante, S.; Facchetti, A.; Pagani, G. A. *J. Org. Chem.* **1997**, *62*, 5755–5765. (b) Abbott, A.; Bradamante, S.; Facchetti, A.; Pagani, G. A.; Ledoux, I.; Zysy, J. *Mater. Res. Soc. Symp. Proc.* **1998**, *488*, 815–818. (c) Abbott, A.; Bradamante, S.; Facchetti, A.; Pagani, G. A.; Yuan, L.; Prasad, P. N. *Gazz. Chim. Ital.* **1997**, *127*, 165–166.

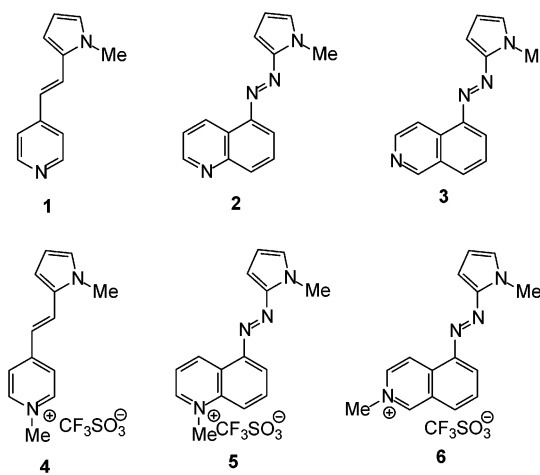
(16) Bradamante, S.; Facchetti, A.; Pagani, G. A. *J. Phys. Org. Chem.* **1997**, *10*, 514–524.

(17) Katritzky, A. R. *Handbook of Heterocyclic Chemistry*; Pergamon Press: Oxford, U.K., 1983.

(18) (a) Ricceri, R.; Abbott, A.; Facchetti, A.; Grando, D.; Gabrielli, G.; Pagani, G. A. *Colloids Surf. A* **1999**, *150*, 289–296. (b) Ricceri, R.; Neto, C.; Abbott, A.; Facchetti, A.; Pagani, G. A. *Langmuir* **1999**, *15*, 2149–2151. (c) Ricceri, R.; Abbott, A.; Facchetti, A.; Pagani, G. A.; Gabrielli, G. *Thin Solid Films* **1999**, *340*, 218–230. (d) Ricceri, R.; Grando, D.; Abbott, A.; Facchetti, A.; Pagani, G. A.; Gabrielli, G. *Langmuir* **1997**, *13*, 5787–5790. (e) Ricceri, R.; Abbott, A.; Facchetti, A.; Pagani, G. A.; Gabrielli, G. *Langmuir* **1997**, *13*, 4182–4184. (f) Ricceri, R.; Abbott, A.; Facchetti, A.; Pagani, G. A.; Gabrielli, G. *Langmuir* **1997**, *13*, 3434–3437.

optical limiting activities via two-photon absorption process.<sup>20</sup>

Following the above strategy, we show here that molecules **1**–**3** are suitable precursors for the synthesis



of push–pull/donor–acceptor salts **4**–**6** of type **I** and for their subsequent incorporation in self-assembled polar monolayers **7**–**9**.

The azine heterocycle acceptors are found to have a dominant influence on the overall azinium–(π-bridge)–pyrrole chromophore properties, both in solution and in the solid state as noncentrosymmetric thin films. Finally, it is shown that the pyrrol-2-yl substituent exhibits a donor capacity similar to that of primary organic functionalities such as amino, dialkylamino, and hydroxy in both stilbene and stilbazolium-based NLO-phores.

## Results and Discussion

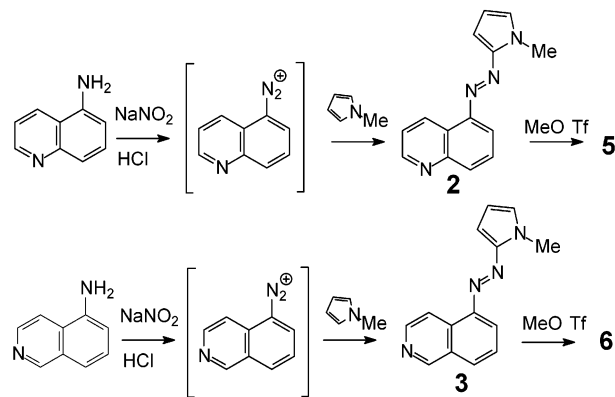
**Chromophore Preparation and Characterization.** *Synthesis.* Chromophore precursors **2** and **3** and the corresponding *N*-methotriflates **5** and **6** were conveniently prepared according to Scheme 1. Diazotation of 5-aminoquinoline and 5-aminoisoquinoline with  $\text{HNO}_2$  in water afforded the corresponding diazonium salts, which were immediately reacted with *N*-methylpyrrole to afford **5** and **6** in very good yields (~80%). We previously described<sup>16</sup> the preparation of salt **4** from the pyridine-based system **1**. Similarly, the new azinium salts **5** and **6** were prepared in excellent yields (>95%) by methylation of the azine precursors **2** and **3** using methyl triflate in benzene.

The preparation of the azo analogue of **4** was also initially envisioned to have a straightforward comparison with chromophores **5** and **6** and known stilbazolium-

(19) (a) Facchetti, A.; van der Boom, M. E.; Abbotto, A.; Beverina, L.; Marks, T. J.; Pagani, G. A. *Langmuir* **2001**, *17*, 5939–5942. (b) Pagani, G. A.; Abbotto, A.; Beverina, L.; Bradamante, S.; Facchetti, A.; van der Boom, M. E.; Marks, T. J. *Polym. Prepr.* **2001**, *42*, 567–568.

(20) (a) Abbotto, A.; Beverina, L.; Bozio, R.; Facchetti, A.; Pagani, G. A.; Ferrante, C.; Pedron, D.; Signorini, R. *Org. Lett.* **2002**, *4*, 1495–1498. (b) Abbotto, A.; Beverina, L.; Bozio, R.; Bradamante, S.; Pagani, G. A.; Signorini, R. *Synth. Met.* **2001**, *121*, 1755–56. (c) Abbotto, A.; Beverina, L.; Bozio, R.; Bradamante, S.; Ferrante, C.; Pagani, G. A.; Signorini, R. *Adv. Mater.* **2000**, *12*, 1963–1967. (d) He, G. S.; Yuan, L. X.; Prasad, P. N.; Abbotto, A.; Facchetti, A.; Pagani, G. A. *Opt. Commun.* **1997**, *140*, 49–52.

**Scheme 1. Synthetic Protocol for the Synthesis of Chromophores **5** and **6****



and disperse red-like dyes. The key intermediate for its preparation is the system **1**-AZO, structure shown in Scheme 2.

Unfortunately, all of our efforts to isolate this compound have so far unsuccessful. In all probability, the diazonium salt of 4-aminopyridine undergoes rapid nitrogen elimination,<sup>21</sup> affording 4-hydroxy or 4-halopyridines, depending on the acid used in the reaction.<sup>22</sup> Therefore, starting from 4-aminopyridine, isoamyl nitrite, and  $\text{NaNH}_2$ , the stable pyridine-4-diazotate sodium salt was isolated and then reacted with *N*-methylpyrrole under acidic conditions. This approach did not afford the desired **1**-AZO molecule either.

*UV–Visible/PL Spectroscopy.* Table 1 collects UV–visible optical spectroscopic data ( $\lambda_{\text{max}}$ ,  $\epsilon$ ) for **1**–**6** in methanol and either toluene or water. From previous studies on azine–(C=C)–π-excessive heterocycle systems such as **1**,<sup>16</sup> azine precursors **2** and **3** were expected to exhibit marginal push–pull activity. On the other hand, alkylation of the azine nitrogen atom to afford the corresponding azinium derivatives is found to have large influence on chromophore optical properties. Indeed, chromophores **4**–**6** experience a bathochromic shift ( $\Delta\lambda_n^+$ )<sup>23</sup> compared to the neutral precursors **1**–**3**, due to the much stronger acceptor capacities of azinium versus azine groups. In methanol, this effect is much larger for the pyridine-based derivatives ( $\Delta\lambda_n^+ = 82$  nm for **1**–**4**) than for the quinoline ( $\Delta\lambda_n^+ = 53$  nm for **2**–**5**) and isoquinoline ( $\Delta\lambda_n^+ = 18$  nm for **3**–**6**) systems. The established correlation between donor/acceptor strength and  $\Delta\lambda_n^+$ <sup>16</sup> suggests that intramolecular charge transfer (ICT) from the pyrrol-2-yl donor group is better promoted by the 4-pyridinium ring. This effect is small with the other two benzofused azinium acceptors and is explicable considering the different effect of the ICT (**a** → **b**, **c** in Scheme 3) on **4** versus **5** and **6**. In fact, intramolecular charge transfer from the pyrrole ring to the azine group corresponds to a switch from an aromatic-like (**a**) to a quinoid-like (**b** or **c**) limit structure. In contrast to **4**, in the case of chromophores **5** and **6**, not only the azine ring but also the annellated

(21) (a) Albert, A.; Ritchie, B. *J. Chem. Soc.* **1943**, 458–461. (b) Morgan, T. J.; Walls, L. P. *J. Chem. Soc.* **1932**, 2227–2231.

(22) (a) March, J. *Advanced Organic Chemistry*; Wiley: New York, 1985. (b) Perker, E. D.; Shire, W. *J. Am. Chem. Soc.* **1947**, *69*, 63–72.

(23) The parameter  $\Delta\lambda_n^+ = (\lambda_{\text{max}}^{\text{cation}} - \lambda_{\text{max}}^{\text{neutral}})$  is defined as the difference between the ICT band value of the methylazinium ion and that of the corresponding azine base. See ref 16.

Scheme 2. Synthetic Attempts to Chromophore 1-AZO

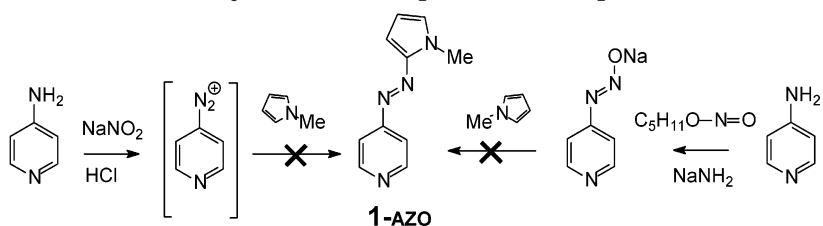
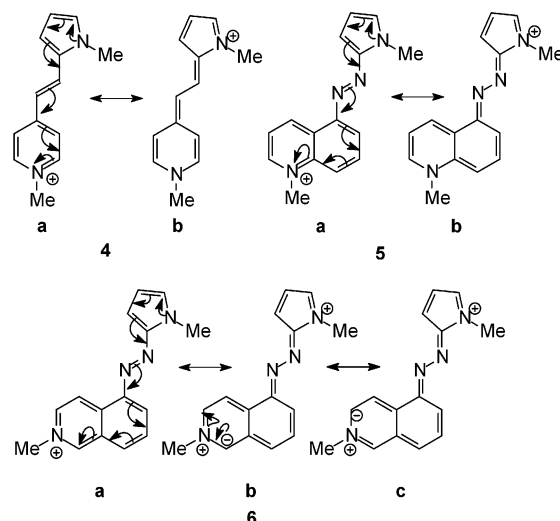


Table 1. Long-Wavelength UV-Visible Optical Absorption Maximums of 1-6 in Various Solvents and as Self-Assembled Films 7-9

compd	toluene	MeOH ( $\epsilon$ ) <sup>b</sup>	H <sub>2</sub> O	film	$\Delta\lambda_{\text{solv2}}^{\text{solv1}}\text{a}$
<b>1</b>	356	362 <sup>c</sup> (21 100)			+6
<b>4</b>		444 <sup>c</sup> (32 200)	422 <sup>c</sup>		-22
<b>7</b>			448		
<b>2</b>	414	412 (22 100)			-2
<b>5</b>		465 (51 100)	457		-8
<b>8</b>			477		
<b>3</b>	416	415 (14 150)			-1
<b>6</b>		433 (16 100)	428		-5
<b>9</b>				455	

<sup>a</sup>  $\Delta\lambda_{\text{solv2}}^{\text{solv1}} = \lambda_{\text{max}} \text{ (solvent 1)} - \lambda_{\text{max}} \text{ (solvent 2)}$ , with dielectric constants  $\epsilon_1 > \epsilon_2$ ; positive  $\Delta\lambda$  means positive solvatochromism.  
<sup>b</sup> Extinction coefficient  $\epsilon$  in L mol<sup>-1</sup> cm<sup>-1</sup>. <sup>c</sup> From ref 16.

Scheme 3. Aromatic (a), Quinoid (b), and (c) Resonance Structures of Chromophores 4-6



benzene ring loses aromaticity upon ICT. The net effect is an enhanced tendency of the azine group to accept charge in **4** than in **5** and **6**. Within the latter two systems, the acceptor tendency of the 5-quinolinium fragment is larger than that of the 5-isoquinolinium group, probably because **5** can delocalize  $\pi$ -charge directly from the pyrrole donor to the positive nitrogen atom acceptor. On the other hand, the 5-isoquinolinium group in **6** can only locate charge on the carbon atoms adjacent the positively charged nitrogen atom (formulas **b** and **c**), but not directly on it.

The solvatochromic response ( $\Delta\lambda_{\text{solv2}}^{\text{solv1}}$ ), which reflects the ability of the solvent to stabilize ICT, also supports the above results. Thus, the measured  $\Delta\lambda_{\text{solv2}}^{\text{solv1}}$  in toluene/methanol and methanol/water pairs for neutral systems **1-3** and salts **4-6**, respectively, are reported in Table 1. The extent of  $\Delta\lambda_{\text{solv2}}^{\text{solv1}}$  is found to be 3-5 times larger in **4-6** than in **1-3**. Among the salts, **4**

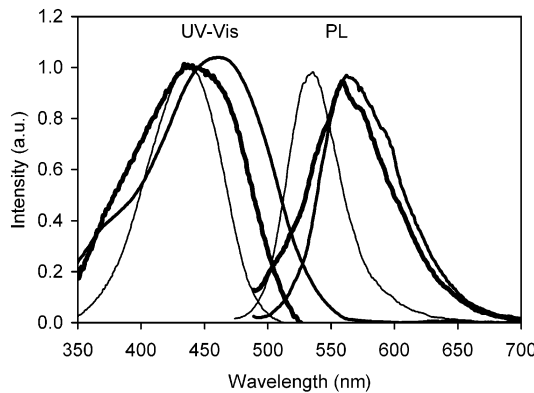


Figure 1. Optical absorption (UV-visible) and emission (PL) spectra of **4** (thin line), **5** (middle line), and **6** (thick line) in DMSO at 25 °C. Solution PL excitation at the long-wavelength absorption maximums. Intensities are in arbitrary units.

Table 2. Optical Emission Data (Fluorescence Maximums,  $\lambda_f$ , and Quantum Yield,  $\Phi_f$ )<sup>a</sup> of 4-6 and Self-Assembled Films 7-9

compound	solvent	$\lambda_{\text{exc}}$ (nm)	$\lambda_f$ (nm)	$\Delta\lambda$ (nm) <sup>b</sup>	$\Phi_f$	$E_{\text{ge}}$ (eV) <sup>c</sup>
<b>4</b>	MeOH	438	518	80	0.02	2.51
<b>4</b>	DMSO	437	532	95	0.22	2.52
<b>7</b>		448	525	77		2.48
<b>5</b>	DMSO	467	558	91	0.12	2.36
<b>8</b>		477	545	68		2.43
<b>6</b>	DMSO	444	555	111	0.15	2.46
<b>9</b>		455	543	88		2.47

<sup>a</sup> 9,10-Diphenylanthracene was used as standard ( $\Phi_f = 0.90$  in cyclohexane). <sup>b</sup> Stark shift. <sup>c</sup> Optical gap.

clearly exhibits the largest response. In general, sizable solvatochromic responses are indicative of highly polarizable  $\pi$ -electron structures. These features are key factors in designing efficient second-order NLO phores. Therefore, the UV-visible optical data suggest that chromophore **4** is expected to have a greater hyperpolarizability than **5** and **6**.

Figure 1 shows optical (UV-visible) absorption and emission (PL) spectra of chromophores **4-6** in DMSO, and Table 2 summarizes emission data in anhydrous methanol, DMSO, or both for all of the chromophores. Quaternization of azine nitrogen also has a dramatic influence on the fluorescence properties of these heterocycle-based systems. In fact, **1-3** have no appreciable emission when excited at their absorption maximums, whereas the corresponding salts **4-6** and monolayers **7-9** (vide infra) emit in the visible region (518-558 nm). The highest quantum efficiency<sup>24</sup> ( $\Phi_f = 0.22$ ) was found for pyridinium system **4** in DMSO, while **5** and **6** exhibit somewhat lower values ( $\Phi_f = 0.12$  and 0.15, respectively). In general  $\Phi_f$  is 1-2 orders of magnitude greater

in DMSO than in MeOH. Combining absorption and emission data, the HOMO–LUMO (optical) energy gap can be estimated and is found to be in the range of 2.4–2.5 eV for all of the present chromophores in solution. Comparable values are found for the corresponding SA films (vide infra).

The spectroscopic UV–visible/PL data, which exhibit very similar HOMO–LUMO separations ( $E_{\text{ge}}$ ) in chromophores **4–6**, indicate that the stronger acceptor capacity of pyridinium ring in **4**, as evidenced by the greater  $\Delta\lambda_{n^+}$  and  $\Delta\lambda_{\text{solv}1}^{\text{solv}2}$  parameters, compensates for the more extended  $\pi$ -core of chromophores **5** and **6** in terms of  $\pi$ -conjugation. According to the two-state model,<sup>25</sup> for molecular systems exhibiting a dominant ICT transition, the major component of the  $\beta$ -tensor is given by eq 1

$$\beta = k (\Delta\mu \mu_{\text{eg}}^2) / E_{\text{ge}}^2 \quad (1)$$

where  $k$  is a constant that depends on the convention used,<sup>26</sup>  $\Delta\mu = (\mu_e - \mu_g)$  is the difference between the excited and ground-state dipole moments, and  $\mu_{\text{eg}}$  is the transition dipole moment. The latter parameter can be calculated from the charge-transfer band of the chromophores.<sup>27</sup> Comparable  $\mu_{\text{eg}}$  values of  $25 \times 10^{-30}$ ,  $33 \times 10^{-30}$ , and  $18 \times 10^{-30}$  C·m are found for **4–6**, respectively. In conclusion, if **4** is found to exhibit the largest NLO response among the present salts, as suggested by the UV–visible data, this is certainly due to a larger molecular polarization and therefore greater  $\Delta\mu$ .

**Electrochemical Studies.** The electronic consequences of nitrogen alkylation were also investigated by cyclic voltammetry (one-compartment cell with Pt working electrode, Ag/0.1 M AgNO<sub>3</sub> (CH<sub>3</sub>CN) reference, Ag counter electrode).<sup>28</sup> Voltammograms of  $\sim 10^{-3}$  M CH<sub>3</sub>CN solution of **1–3** (0.10 M TBABF<sub>4</sub> electrolyte) exhibit a single chemically irreversible oxidative wave at +0.99, +1.14, and +1.17 V, respectively, and negligible reductive features, indicating chemically irreversible oxidative processes. Figure 2 shows representative voltammograms for **2** and **5**. After alkylation, dyes **4–6** show both irreversible oxidative (+1.18, +1.45, and +1.33 V, respectively) and reductive (-1.19, -0.82, and -1.01 V) waves. Note that the first anodic peaks of **4–6** versus **1–3** exhibit an anodic shift ( $\sim +0.2$ –0.3 V), indicating that alkylation/quaternization of the aromatic core substantially increases the ionization potential. In addition, the enhanced electron-acceptor properties of **4** and **5** are also supported by the appearance of reductive waves. HOMO–LUMO (electrochemical) gaps can be estimated from the oxidation and reduction potentials. We are aware that a precise  $E_{\text{g}}$  determination requires knowledge of the standard potentials.<sup>29</sup> However, from the present oxidative/reductive data, we estimate HOMO–LUMO gaps of  $\sim 2.4$  and 2.3 eV for **4** and **5**, **6**, respectively, in very good agreement with the optical gaps.

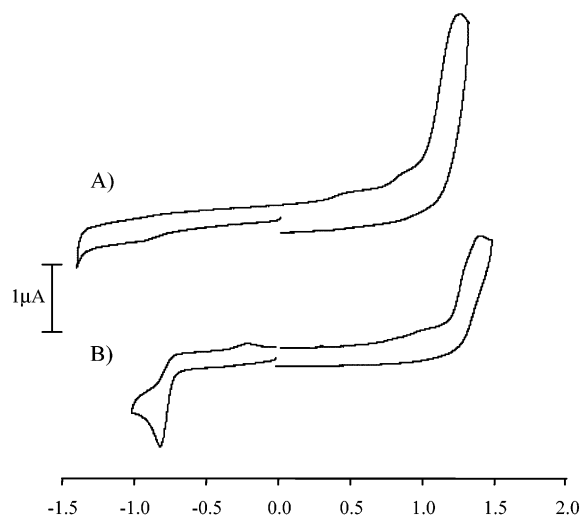


**Figure 2.** Cyclic voltammogram (first scan,  $v = 100$  mV/s) in acetonitrile on a 0.8-mm-diameter glassy carbon electrode at 25 °C. (A) Chromophore precursor **2**. (B) Chromophore **5**.

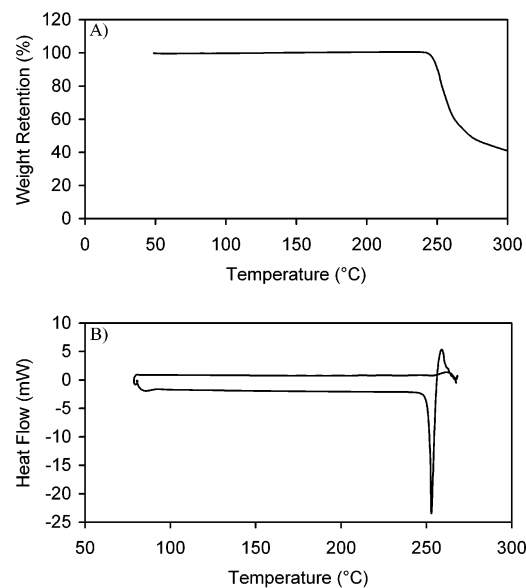


**Figure 3.** Thermal analysis data for chromophore **4**. (A) TGA trace recorded under reduced pressure (0.01 Torr N<sub>2</sub>) at a ramp rate of 1.5 °C/min. (B) DSC trace at a heating rate of 10 °C/min under nitrogen.

**Thermal Data.** The comparative thermal properties of **3–6** were investigated by DSC and TGA. Figure 3 shows TGA (A) and DSC (B) traces for chromophore **4**. DSC profiles of **4** and **5** show a distinct crystal-to-isotropic transition at 251 and 207 °C respectively, close to their observed capillary melting points (see Experimental Section). After melting, exothermic transitions centered at 260 and 223 °C are detected, which can be associated with decomposition processes. Compound **6** does not show any endothermic peaks but only a strong exothermic transition at 228 °C. The sizable exergonic peaks of **5** and **6**, compared to that of **4**, are probably due to decomposition reactions leading to very stable products such as dinitrogen. This result is not unexpected in view of the chromophore molecular structures. All of the chromophore TGA plots exhibit negligible weight loss below 250 °C for **4** and 200 °C for **5** and **6**. Both DSC and TGA data suggest that all of the present chromophores are quite thermally stable up to their

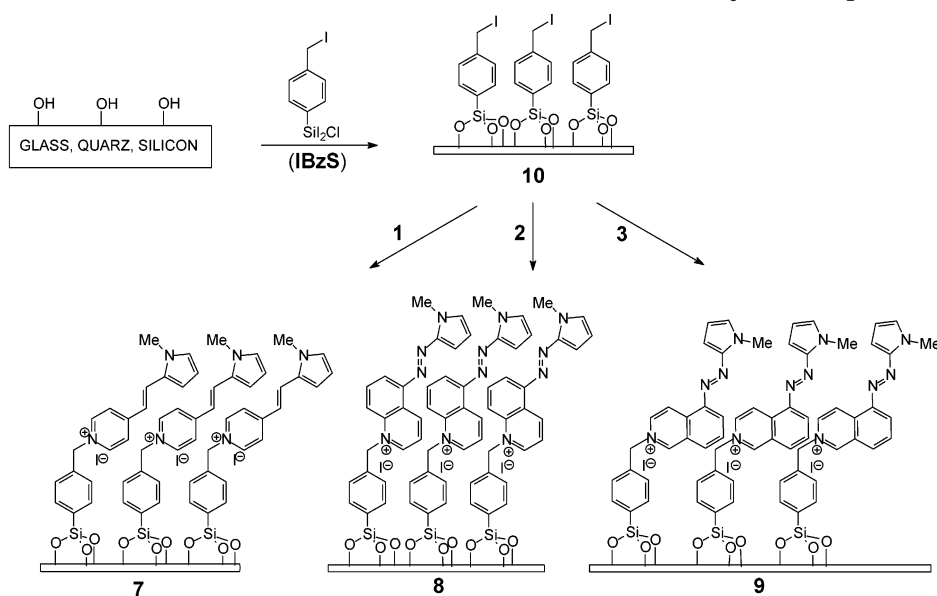
(25) Oudar, J. L.; Chemla, D. S. *J. Chem. Phys.* **1977**, *66*, 2264–2268.

(26) Willets, A.; Rice, J. E.; Burland, D. M.; Shelton, D. P. *J. Chem. Phys.* **1992**, *97*, 7590.

(27) Atkins, P. W. *Physical Chemistry*; Freeman Co.: New York, 1994.

(28) The Ag/AgNO<sub>3</sub> reference electrode was additionally calibrated against ferrocene/ferrocinium ( $E_{1/2} = 0.042$  V).

(29) Bard, A. J.; Faulkner, L. R. *Electrochemical Methods—Fundamentals and Applications*; Wiley: New York, 1984.

**Scheme 4. Construction of Films 7–9 via Self-Assembly Techniques**

melting points. Therefore, self-assembled films based on these kinds of structures are expected also to exhibit high thermal stability. Importantly, the SA technique for the preparation of films **7–9** requires thermally robust chromophore precursors (vide infra) and the TGA plots of **1–3** indicate that these systems are stable in the film deposition range (110–120 °C) well beyond the time required (20–30 min) for quantitative coupling to the surface.

**Film Fabrication and Characterization.** *Film Fabrication.* The incorporation of the azine-based chromophores **1–3** into self-assembled acentric films was achieved via a two-step, self-limiting chemisorptive siloxane condensation process (Scheme 4). In the first step, clean substrates possessing a hydroxylated surface undergo reaction with the *p*-(iodomethyl)phenyldiiodochlorosilane (IBzS) coupling reagent to afford the benzyl halide-functionalized monolayer **10**. Chromophore precursors **1–3** are then coupled to the substrate through quaternization at the azine nitrogen atom with the benzyl halide coupling agent. However, benzofused systems **2** and **3** require, compared to **1**, precise control of the experimental conditions to furnish the corresponding films. Higher oven temperatures (>120 °C) or dynamic vacuum precludes chromophore film formation (see Experimental Section). This is probably due to the greater volatility of **2** and **3** compared to **1**. On the other hand, at lower reaction temperatures (<100 °C), reactions appear to be inhibited by the lower reactivity of the benzofused systems, in particular quinoline, compared to that of the pyridine-based precursor. All of the SA films were characterized by UV-visible/PL spectroscopies, atomic force microscopy (AFM), advancing aqueous contact angle (CA) measurements, specular X-ray reflectivity (XRR), and second harmonic generation (SHG) measurements. These techniques confirm that a densely packed chromophore layer is formed via nucleophilic substitution at the azine nitrogen by the covalently bonded iodobenzyl-functionalized monolayer.

**UV-Vis/PL Spectroscopy.** The coupling layer is covalently bonded to the substrate surface via siloxane linkages. After attachment of the chromophore to the

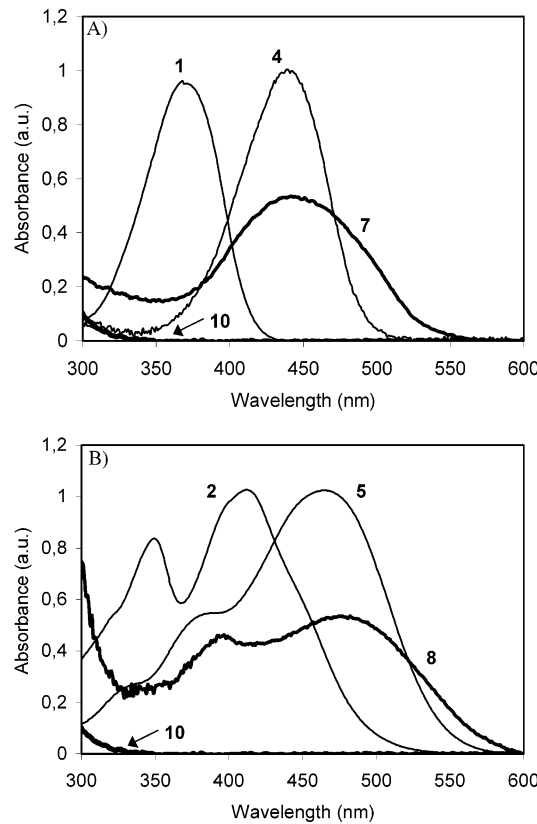


**Figure 4.** Transmission optical absorbance spectra (a.u., arbitrary units). (A) Pyridine-based chromophore precursor **1** in MeOH, the corresponding methotriflate **4** (in MeOH), IBzS coupling film **10**, and film **7**. (B) Quinoline-based chromophore precursor **2** in MeOH, the corresponding salt **5** (in MeOH), IBzS coupling film **10**, and film **8**.

coupling layer, a characteristic change in the optical spectrum is observed (Figure 4). The coupling layer **10** exhibits no significant absorption at wavelengths greater than 300 nm. After reaction with **1–3**, a characteristic intrachromophore charge-transfer band (Table 1) is observed. This band is red-shifted in comparison not only with the features of **1–3** but also with respect to the corresponding dyes **4–6** in solution. This shift in

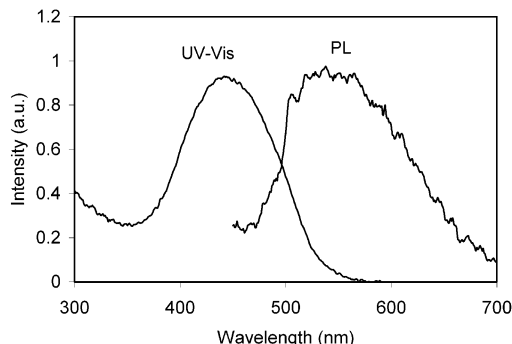


**Figure 5.** Optical absorption (UV–visible) and emission (PL) spectra of film 7 at 25 °C. Intensities are in arbitrary units.

optical absorption can be attributed to conversion of the pyridyl group into a pyridinium group, confirming the quaternization reaction on the surface. The film chromophore densities ( $N_s$ ) can be estimated<sup>30</sup> from absorption spectra of **7–9** and using the extinction coefficient of **4–6** in solution (Table 1). Comparable  $N_s$  values of  $\sim 3 \times 10^{14}$ ,  $2 \times 10^{14}$ , and  $5 \times 10^{14}$  molecule/cm<sup>2</sup> are estimated for **4–6**, respectively, in accord with previously reported SA chromophores<sup>31</sup> and indicating comparably dense packing.

Additionally, the present heterocycle-based chromophores still exhibit fluorescence characteristics as thin films when excited at the absorption maximums. Figure 5 shows UV–visible/PL spectra of film 7. Although quantitative PL measurements were not performed, from the relative film UV–visible/PL absorption/emission intensities, chromophore **7** is estimated to be roughly 1 order of magnitude more efficient than **8** and **9**. Maintenance of fluorescence properties in thin films level may also enable efficient up-converted lasing via two-photon absorption.<sup>32</sup> Studies in this direction are currently in progress.

**Atomic Force Microscopy.** Figure 6A shows the AFM image of a IBnS self-assembled monolayer **10** on a single-crystal Si(111) substrate. Topologically, this coupling layer is essentially featureless and extremely smooth with an root-mean-square (rms) roughness of  $\sim 2.2$  Å for a scan area of  $0.5 \times 0.5 \mu\text{m}^2$ . AFM images show no indication of island growth or film cracking, suggesting that the coupling agent is deposited as a smooth, uniform, continuous film. Similar results were obtained on ClBnS-based<sup>33</sup> SA monolayers<sup>31</sup> and well-ordered LB films.<sup>7a</sup> Upon reaction of the coupling layer with **1**, a self-assembled bilayer structure is formed according to Scheme 3. The AFM image for the film **7** is shown in Figure 6B. This image also demonstrates good film quality with a continuous surface having only a slight increase in the rms roughness to  $\sim 2.5$  Å.

(30)  $N_s = A/2\epsilon$  since the chromophores are assembled on both sides of the glass substrate. This is a rough estimation of the surface coverage since it is assumed that the chromophore extinction coefficient in solution can be used for the self-assembled chromophore. For an excellent description of the relationship between surface coverage, absorbance, and molecular orientation for polar monolayers, see: Buscher, C. T.; McBranch, D.; Li, D. *J. Am. Chem. Soc.* **1996**, *118*, 2950–2953. For an alternative approach to estimate the surface coverage by UV–visible, see: Moon, J. H.; Shin, J. W.; Kim, S. Y.; Park, J. W. *Langmuir* **1996**, *12*, 4621–4624.

(31) Lin, W.; Lin, W.; Wong, G. K.; Marks, T. J. *J. Am. Chem. Soc.* **1996**, *118*, 8034–8042.

(32) Marder, S.; Perry, J. U.S. Patent 6,267,913, 2001; *Chem. Abstr.* **2001**, *135*, 159952.

(33) ClBnS stands for *p*-(chloromethyl)phenyliodiodochlorosilane.

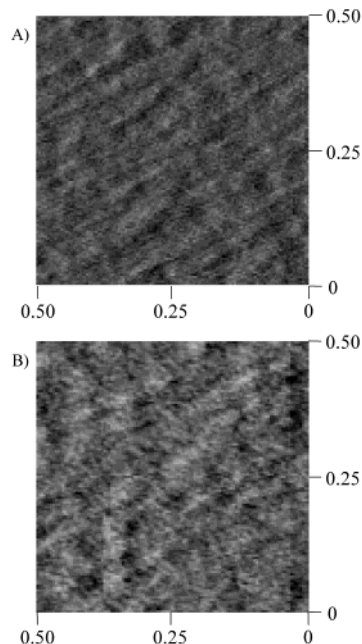


**Figure 6.** AFM images at  $0.5 \times 0.5 \mu\text{m}^2$  scan areas on a Si(111) substrate. (A) Coupling layer film **10**. (B) Self-assembled chromophoric film **7**.

Analogous, featureless images were obtained for SA films **8** and **9** exhibiting rms roughnesses of  $\sim 2.8$  and  $3.1$  Å, respectively.

**Advancing Contact Angle Measurements.** Further evidence for the formation of films **7–9** as depicted in Scheme 4 is obtained from aqueous advancing CA measurements. Clean glass slides exhibit very low contact angle values ( $\theta_a < 5^\circ$ ), while iodobenzyl-functionalized surface **10** exhibits a significant increase in  $\theta_a$ , reaching  $71 \pm 4^\circ$ , in accord with a dense coupling layer surface coverage. After reaction with chromophore precursors **1–3**, self-assembled iodide salts are formed on the surface. This should yield a more polar surface, and indeed, the corresponding films exhibit a lower  $\theta_a$  values of  $46 \pm 2$ ,  $51 \pm 4$ , and  $55 \pm 4^\circ$  for **7–9** respectively.

**XRR Measurements.** To further characterize the self-assembled films **7–9** and to get insight into the film microstructural details, X-ray reflectivity measurements were performed on these structures grown on the native oxide surface of single-crystal Si(111). Figure 7 shows X-ray reflectivity data normalized to the Fresnel reflectivity for self-assembled bilayer **7**. The reflected intensity was measured as a function of the scattering vector perpendicular to the reflecting surface (specular reflectivity). Fitting of the specular reflectivity data to the Gaussian-step model gives (i) the film electron density profile or average electron density of the film ( $\rho_{\text{film}}$ ), (ii), the thickness of film ( $d$ ), and (iii) the rms width of each interface ( $\sigma_{\text{film-air}}$ ), which corresponds to the film roughness (Table 3). The chromophore number density ( $N_s$ ) can also be calculated from the amount of electrons per unit area for one molecular layer. The latter can be obtained from the experimental electron density profile and the number of electrons for each SA molecule calculated from the chemical formula of films **7–9**. A detailed description of the XRR data analysis and models can be found elsewhere.<sup>34</sup> The XRR data suggest that film **8** is thicker than **7** and **9**. Indeed, this result

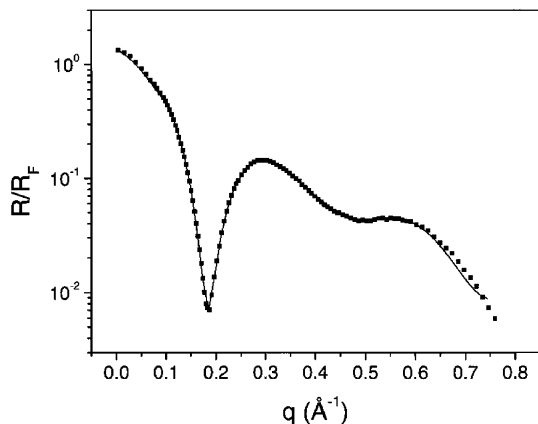


**Figure 7.** X-ray reflectivity data normalized to the Fresnel reflectivity  $R_F$  plotted versus wave vector for film 7.

**Table 3. Specular XRR Data<sup>a</sup> for Self-Assembled Films 7–9**

film	$\rho_{\text{film}}$ (electrons/Å <sup>3</sup> )	$d$ (Å)	$\sigma_{\text{film-air}}$ (Å)	$N_s$ (molecule/cm <sup>2</sup> )
7	$0.26 \pm 0.02$	$15.3 \pm 0.1$	$3.6 \pm 0.1$	$2.1 \times 10^{14}$
8	$0.27 \pm 0.01$	$19.9 \pm 0.2$	$4.3 \pm 0.2$	$2.6 \times 10^{14}$
9	$0.22 \pm 0.01$	$15.6 \pm 0.1$	$3.3 \pm 0.2$	$1.9 \times 10^{14}$

<sup>a</sup>  $\rho_{\text{film}}$ , electron density;  $d$ , film thickness;  $\sigma_{\text{film-air}}$ , film roughness;  $N_s$ , chromophore density.

is expected in view of the film molecular arrangements (see Scheme 4). In addition, the thickness trend is in good agreement with molecular modeling computations.<sup>35</sup> Film roughness is comparable to that obtained via AFM. Finally,  $N_s$  values determined from optical absorption data are slightly larger than those found from the XRR measurements. However, both methods provide evidence that **7–9** chromophore density is similar for all of the films.

Two conclusions can be drawn from these results. First, under specific temperature and pressure conditions, precursors **1–3** undergo reaction with iodobenzyl-functionalized surfaces to afford comparable chromophore coverages, *independent* of the azine nucleophile (pyridine, quinoline, isoquinoline). Second, since there is roughly the same number of chromophore units with similar orientation on the substrate surface, a bulk observable such as  $\chi^{(2)}_{\text{zzz}}$  can be straightforwardly related to  $\beta$ , a molecular level property (vide infra).

**Second Harmonic Generation Measurements.** Regarding the microstructure of the self-assembled chromophore layers, polarized SHG measurements provide convincing evidence of net polar chromophore alignment with respect to the surface normal. Figure 8 shows the intensity of second harmonic light generated as a function of incident angle from the interaction of a

(34) Evmenenko, G.; van der Boom, M. E.; Kmetko, J.; Dugan, S. W.; Marks, T. J.; Dutta, P. *J. Chem. Phys.* **2001**, *115*, 6722–6727.

(35) Semiempirical computations (MOPAC 6.0: Stewart, J. J. P. *QCPE* **455**, **1990**; keywords PM3, EF, PRECISE) were carried out on model systems of the films **7–9** formed by one chromophore and one coupling unit ending with a Si(OH)<sub>3</sub> group. Calculations were performed on the free azinium salts with no symmetry constraints (symmetry point group  $C_1$ ). We used two different starting geometries corresponding to the two conformers arising from the transoid and cisoid arrangement along the bond between the pyrrolyl C(2) atom and the central double bond unit. The transoid conformer was found to be the most stable by 0.2, 2.2, and 2.4 kcal mol<sup>-1</sup> for **7–9**, respectively. The molecular lengths associated to these geometries are 16.49 and 17.28 Å for **7** and **9**, respectively, and 18.01 Å for **8**.

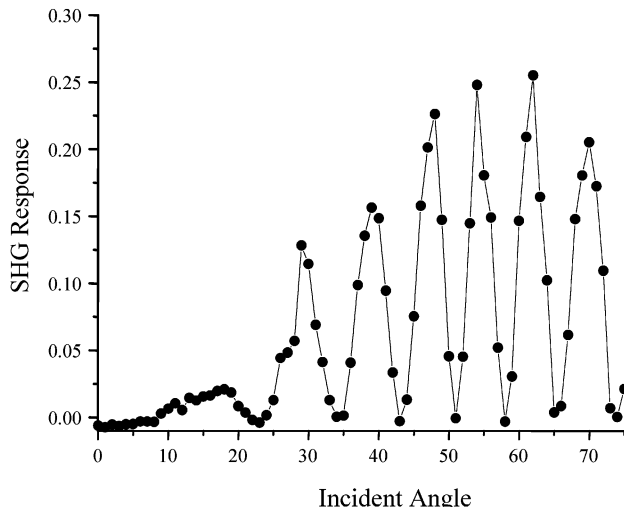


**Figure 8.** Intensity of SHG signal (arbitrary units) as a function of the fundamental beam incident angle from a float glass slide having self-assembled film of **7** on either side.

$\lambda_0 = 1064$  nm incident laser beam with a glass slide coated on both sides with a self-assembled bilayer, **7**. The “rocking” of the substrate results in a characteristic SHG interference pattern arising from the phase difference between the two SHG waves generated at either side of the sample. The presence of near-zero intensity minimums in Figure 8 indicates that the quality and uniformity of the deposited films on each side of the substrate is nearly identical. By calibrating the angle-dependent SHG data against quartz, a bulk second-order nonlinear susceptibility  $\chi^{(2)}_{\text{zzz}}$  of  $34 \times 10^{-8}$  (142 pm/V),  $1.6 \times 10^{-8}$  (6.7 pm/V), and  $1.3 \times 10^{-8}$  esu (5.4 pm/V) are obtained for self-assembled films **7–9**, respectively. These NLO responses doubtless arise from the chromophore layer since the  $\chi^{(2)}_{\text{zzz}}$  response of a coupling layer such as **10** (ClBnS instead of IBnS) is in the range of  $(2–3) \times 10^{-9}$  esu.<sup>36</sup> The electrooptic coefficient  $r_{33}$  can be related to  $\chi^{(2)}_{\text{zzz}}$  by the approximate relationship  $r_{33} = -2\chi^{(2)}_{\text{zzz}}/n$ ,<sup>4</sup> where  $n$  is the index of refraction of the film.<sup>6c,37</sup> Reasonably assuming an index of refraction of 1.6 for self-assembled organic films of this type,<sup>38</sup>  $r_{33}$  estimates of 44, 2.0, and 1.6 pm/V are obtained for **7–9**, respectively. Electrooptic response of pyridine-based film **7** is comparable to those of other high-efficient organic-based films<sup>39</sup> and is significantly higher than inorganic material such as LiNbO<sub>3</sub>.<sup>40</sup> Note that these values were obtained under nominally non-resonant conditions<sup>41</sup> since none of these chromophores absorb significantly at 532 nm (2ω).

(36) Huang, W.; Helvenston, M. *Langmuir* **1999**, *15*, 6510–6514.

(37) Ashley, P. R.; Cites, J. S. *Opt. Soc. Am. Technol. Dig. Ser.* **1997**, *14*, 196–200.

(38) (a) Lin, W.; Lee, T. L.; Lyman, P. F.; Lee, J. J.; Bedzyk, M. J.; Marks, T. J. *J. Am. Chem. Soc.* **1997**, *119*, 2205–2211.

(39) (a) Penner, T. L.; Motschmann, H. R.; Armstrong, N. J.; Ezenyilimba, M. C.; Williams, D. J. *Nature* **1994**, *367*, 49–51. (b) Robinson, B. H.; Dalton, L. R.; Harper, A. W.; Ren, A.; Wang, F.; Zhang, C.; Todorova, G.; Lee, M.; Anisfeld, R.; Garner, S.; Chen, A.; Steier, W. H.; Houbrech, S.; Persoons, A.; Ledoux, I.; Zyss, J.; Jen, A. K. Y. *Chem. Phys.* **1999**, *245*, 35–50.

(40) Dalton, L. R.; Steier, W. H.; Robinson, B. H.; Zhang, C.; Ren, A.; Garner, S.; Chen, A. T.; Londergan, T.; Irwin, L.; Carlson, B.; Fifield, L.; Phelan, G.; Kincaid, C.; Amend, J.; Jen, A. *J. Mater. Chem.* **1999**, *9*, 1905–1920.

(41) Lundquist, P. M.; Yitzchaik, S.; Zhang, T.; Kanis, D. R.; Ratner, M. R.; Marks, T. J.; Wong, G. K. *Appl. Phys. Lett.* **1994**, *64*, 2194–2197.

The present SHG measurements clearly show the greater response of **7** compared to **8** and **9**. These disparities certainly reside in the different natures of the heterocycle acceptors, since previous studies have shown that substitution of  $-\text{C}=\text{C}-$  for  $-\text{N}=\text{N}-$  spacer groups has only a minor influence on the second-order NLO response of such chromophores.<sup>6a,42</sup> In fact, given that films **7–9** have similar chromophore densities and optical absorption maximums, the first hyperpolarizability  $\beta$  of **4** is reasonably estimated to be nearly 2 orders of magnitude greater than those of the other two salts. These data demonstrate that the 4-pyridinium substituent is the most effective acceptor among the azinium groups examined. The large response of **7**, and therefore **4**, is of particular importance since, for the first time, the large donor efficiency of the pyrrol-2-yl group has been experimentally demonstrated. In concurrence with these observations, Marks and Ratner predicted, on the basis of semiempirical electronic structure computations, the importance of the *auxiliary* donor/acceptor effects of  $\pi$ -excessive and  $\pi$ -deficient heterocycles in push–pull systems.<sup>43</sup> The excellent acceptor capacity of 4-pyridinium moiety is well known, and this heterocycle has been widely employed as a building block in NLO-phores. However, to our knowledge, no experimental evidence of the effect of unsubstituted pyrrole rings on chromophore activity has been reported. In one case,<sup>44</sup>  $\beta$ -values of sulfonyl-substituted pyrrole imino chromophores were measured and found to be quite low, probably because the electron-rich ring was embedded in the acceptor site, counteracting its auxiliary action.<sup>43</sup> The present study also demonstrates that a  $\pi$ -excessive (electron-rich), five-membered ring can act as a *primary* donor group when conjugated with an acceptor of proper strength. Finally, taking into account for **7** both its high  $r_{33}$  value and optical transparency, the  $\pi$ -core structure of chromophore **4** should be the focus for the fabrication of thicker assemblies. We are currently studying SA-multilayer films based on appropriately functionalized **4**-like chromophores.<sup>45</sup>

## Conclusion

This paper describes the synthesis of the novel azinium–( $\pi$ -bridge)–pyrrole push–pull chromophores **4–6**. In these molecules, the acceptor group is an electron-poor heterocycle (pyridine, quinoline, isoquinoline) *N*-methyl salt while the donor group is the electron-rich pyrrole ring. Chromophore properties in solution were investigated by combining optical (UV–visible, PL), electrochemical (CV), and thermal measurements. The results demonstrate the greater electron-acceptor capacities of pyridin-4-yl versus quinol-5-yl and isoquinol-5-yl substituents, resulting in a more polarizable structure for **4** compared to **5** and **6**.

(42) For examples, see: Bosshard, C.; Sutter, K.; Prêtre, P.; Hulliger, J.; Flörsheimer, M.; Kaatz, P.; Günter, P. *Organic Nonlinear Optical Materials*; Gordon and Breach Publishers: Basel, 1995.

(43) Albert, I. D. L.; Marks, T. J.; Ratner, M. A. *J. Am. Chem. Soc.* **1997**, *119*, 6575–6582.

(44) Chou, S.-S. P.; Hsu, G.-T.; Lin, H.-C. *Tetrahedron Lett.* **1999**, *40*, 2157–2160.

(45) Abbotto, A.; Beverina, L.; Bradamante, S.; van der Boom, M.; Facchetti, A.; Marks, T. J.; Pagani, G. A. Presented at the 5th National Meeting on Supramolecular Chemistry, Frascati, Italy, September 2001.

Chromophore precursors **1–3** undergo reaction with iodobenzyl-functionalized surfaces **10** affording polar ordered SHG-active films **7–9**. The surface nucleophilic substitution reaction is confirmed by UV–visible optical spectroscopy, where the large red shifts in the **7–9** film absorption maximums, compared to the corresponding precursors **1–3** in solution, indicated quaternization. In addition, these films conserve the intrinsic chromophore fluorescence behavior. Film formation is further confirmed by advancing aqueous contact angle measurements. AFM and XRR data provide additional evidence of film quality.

Film polar order is unambiguously demonstrated by SHG measurements. Films **7–9** are all NLO-active, although pyridine-based monolayer **7** exhibits a much greater response than the other two films. This is in accord with the more polarizable push–pull/donor–acceptor electronic structure of **4** compared to **5** and **6**, as found in solution-phase data. Therefore, the preparation of electrooptic-active multilayers using the siloxane-based SA technique should involve systems derived from proper functionalization of **4**, with preservation of the  $\pi$ -core structure.

This study demonstrates that conjugation of  $\pi$ -excessive and  $\pi$ -deficient heterocycles can lead to high-hyperpolarizable chromophores. In addition, azine groups react with benzyl iodide-functionalized surfaces to yield self-assembled, covalently bonded films. The ability to form microstructurally regular monolayers is a prerequisite for growing thicker SA films of dimensions suitable for device requirements.

## Experimental Section

**General Information.** All synthetic procedures described below were carried out under a nitrogen atmosphere. All solvents were AR grade obtained from Aldrich. Anhydrous solvents were prepared by continuous distillation over sodium sand, in the presence of benzophenone and under nitrogen or argon, until the blue color of sodium ketyl was permanent. Extracted solutions were dried over  $\text{Na}_2\text{SO}_4$  (4 h). Melting points are uncorrected.  $^1\text{H}$  spectra were recorded on a Bruker 500-MHz spectrometer. UV–visible spectra were recorded with a Varian Cary 1E spectrophotometer. Electrochemical measurements were performed using a BAS Epsilon instrument. Aqueous contact angles were measured on a standard tensiometric bench fitted with a Teflon micrometer syringe (Gilmont Instruments, Inc.). Polarized second harmonic generation measurements were made in the transmission mode by placing the glass slides in the path of the 1064-nm output of a Q-switched p-polarized light from a Nd:YAG laser operated at 10 Hz with a pulse width of 3 ns. The details of this setup can be found elsewhere.<sup>5,11</sup> X-ray reflectivity measurements were performed at Beam Line  $\times$ 23B of the National Synchrotron Light Source. Atomic force microscopic images were recorded using a Nanoscope II microscope with A and D scanners (Digital Instruments, Inc.).

**Materials.** The reagents 5-aminoquinoline, 5-aminoisoquinoline, *N*-methylpyrrole, and methyl triflate were obtained from Aldrich, while *p*-(iodomethyl)phenyldiiodochlorosilane (IBnS) was synthesized according to known procedure.<sup>9a</sup> Chromophores 1-(Pyridin-4-yl)-2-(*N*-methylpyrrol-2-yl)ethene (**1**) and 1-(*N*-methyl-4-pyridinio)-2-(*N*-methylpyrrol-2-yl)ethene iodide (**4**) were prepared according to procedures previously reported.<sup>16</sup>

**Synthesis of 5-[(*N*-Methylpyrrol-2-yl)azo]quinoline (2).** A 0 °C solution of  $\text{NaNO}_2$  (0.48 g, 6.89 mmol) in water (2 mL) was added to a 0 °C solution of 5-aminoquinoline (0.94 g, 7.50 mmol) in a water–concentrated  $\text{H}_2\text{SO}_4$  (4 mL, 6:1 v/v) mixture. The resulting diazonium salt solution was immediately drop-

wise added to a mixture of *N*-methylpyrrole (0.50 g, 6.16 mmol) and AcOK (2.50 g) in ethanol (30 mL) at  $-5^{\circ}\text{C}$ . After stirring for 1 h, the solid was collected, washed twice with water, and dried overnight. Pure product was obtained by sublimation as a brown-orange solid (1.15 g, 4.87 mmol, 79.1% yield): mp 166  $^{\circ}\text{C}$ ;  $^1\text{H}$  NMR ( $\text{CDCl}_3$ )  $\delta$  9.21 (1H, d,  $^3J = 8.44$  Hz), 8.99 (1H, d,  $^3J = 4.22$  Hz), 8.15 (1H, d,  $^3J = 8.28$  Hz), 7.86 (1H, d,  $^3J = 7.62$  Hz), 7.75 (1H, t), 7.52 (1H, dd), 7.01 (1H, d,  $^3J = 2.1$  Hz), 6.87 (1H, d,  $^3J = 4.22$  Hz), 6.36 (1H, dd), 4.04 (3H, s). Anal. Calcd for  $\text{C}_{14}\text{H}_{12}\text{N}_4$ : C, 71.17; H, 5.12; N, 23.71. Found: C, 71.22; H, 5.07; N, 23.97.

**Synthesis of 5-[(*N*-Methylpyrrol-2-yl)azo]isoquinoline (3).** A 0  $^{\circ}\text{C}$  solution of  $\text{NaNO}_2$  (0.95 g, 13.79 mmol) in water (3 mL) was added to a 0  $^{\circ}\text{C}$  solution of 5-aminoisoquinoline (1.87 g, 13.00 mmol) in water-concentrated  $\text{H}_2\text{SO}_4$  (7 mL, 6:1 v/v) mixture. The resulting diazonium salt solution was immediately added dropwise to a mixture of *N*-methylpyrrole (1.00 g, 12.32 mmol) and AcOK (5.00 g) in ethanol (60 mL) at  $-5^{\circ}\text{C}$ . After stirring for 1 h, the orange solid was collected, washed twice with water, and dried overnight. Pure product was obtained after column chromatography on silica gel ( $\text{AcOEt-CHCl}_3$  1:1) as a bright orange solid (2.40 g, 10.15 mmol, 82.4%): mp 129  $^{\circ}\text{C}$  after sublimation;  $^1\text{H}$  NMR ( $\text{CDCl}_3$ )  $\delta$  9.30 (1H, s), 8.70–8.50 (2H, m), 8.00–7.90 (2H, m), 7.66 (1H, t,  $^3J = 7.82$  Hz), 7.52 (1H, dd), 7.01 (1H, d,  $^3J = 1.8$  Hz), 6.89 (1H, d,  $^3J = 4.04$  Hz), 6.34 (1H, dd), 4.04 (3H, s). Anal. Calcd for  $\text{C}_{14}\text{H}_{12}\text{N}_4$ : C, 71.17; H, 5.12; N, 23.71. Found: C, 71.25; H, 4.98; N, 23.55.

**Synthesis of 5-[(*N*-Methylpyrrol-2-yl)azo]-*N*-methylquinolinium Triflate (5).** A solution of methyl triflate (0.175 g, 1.08 mmol) in dry benzene (3 mL) was added to a solution of 5-[(*N*-methylpyrrol-2-yl)azo]quinoline (0.25 g, 1.08 mmol) in the same solvent (12 mL). After stirring overnight at room temperature, the resulting precipitate (0.42 g, 1.04 mmol, 96.2%) was collected and washed with benzene. Recrystallization from an iso-PrOH-MeOH mixture afforded the analytically pure product as a bright orange solid: mp 211  $^{\circ}\text{C}$  (dec);  $^1\text{H}$  NMR ( $\text{DMSO-}d_6$ )  $\delta$  9.97 (1H, d,  $^3J = 8.46$  Hz), 9.60 (1H, d,  $^3J = 5.42$  Hz), 8.48 (1H, d,  $^3J = 8.82$  Hz), 8.33 (1H, d,  $^3J = 8.00$  Hz), 7.24–8.19 (2H, m), 7.58 (1H,  $^3J = 1.56$  Hz), 7.03 (1H, d,  $^3J = 4.13$  Hz), 6.46 (1H, dd), 4.52 (3H, s), 4.03 (3H, s). Anal. Calcd for  $\text{C}_{16}\text{H}_{15}\text{F}_3\text{N}_4\text{O}_3\text{S}$ : C, 48.00; H, 3.78; N, 13.99. Found: C, 48.18; H, 3.78; N, 14.05.

**Synthesis of 5-[(*N*-Methylpyrrol-2-yl)azo]-*N*-methylisoquinolinium Triflate (6).** A solution of methyl triflate (0.347 g, 2.16 mmol) in dry benzene (5 mL) was added to a solution of 5-[(*N*-methylpyrrol-2-yl)azo]isoquinoline (0.50 g, 2.16 mmol) in the same solvent (25 mL). After stirring overnight at room temperature, the resulting precipitate (0.85 g, 2.11 mmol, 97.8%) was collected and washed with benzene. Recrystallization from an iso-PrOH-MeOH mixture afforded the analytically pure compound as a bright orange solid: mp 217  $^{\circ}\text{C}$  (dec).  $^1\text{H}$  NMR ( $\text{DMSO-}d_6$ )  $\delta$  10.06 (1H, s), 9.15 (1H, d,  $^3J = 3.8$  Hz),

8.76 (1H, d), 8.47 (1H, d,  $^3J = 7.99$  Hz), 8.42 (1H, d,  $^3J = 7.72$  Hz), 8.14 (1H, dd), 7.52 (1H,  $^3J = 1.56$  Hz), 7.07 (1H, d,  $^3J = 4.31$  Hz), 6.49 (1H, dd), 4.52 (3H, s), 4.03 (3H, s). Anal. Calcd for  $\text{C}_{16}\text{H}_{15}\text{F}_3\text{N}_4\text{O}_3\text{S}$ : C, 48.00; H, 3.78; N, 13.99. Found: C, 47.89; H, 3.38; N, 13.96.

**SA Film Deposition.** *Substrate Cleaning.* Sodium lime glass, quartz slides ( $1 \times 1 \text{ cm}^2$ ), and silicon substrates were cleaned by immersion in a “piranha” solution ( $\text{H}_2\text{SO}_4$ :30%  $\text{H}_2\text{O}_2$  = 70:30 v/v) at 80  $^{\circ}\text{C}$  for 1 h (warning: *piranha is an extremely strong oxidation reagent*). After being cooled to room temperature, the substrates were rinsed repeatedly with deionized (DI) water and then sonicated in a solution of DI  $\text{H}_2\text{O}$ , 30%  $\text{H}_2\text{O}_2$ , and  $\text{NH}_3$  (5:1:1 v/v) for 45 min. The substrates were then washed with copious amounts of DI  $\text{H}_2\text{O}$  and dried at 115  $^{\circ}\text{C}$  overnight. All substrates were used immediately after cleaning.

**Coupling Layer Formation Using IBnS.** Scheme 4 shows the general strategy for the formation of the self-assembled chromophore monolayers. Under  $\text{N}_2$ , freshly cleaned substrates were loaded into a Teflon sample holder and immersed in a dry toluene solution of IBnS (14 mM) for 1 h at room temperature. The colorless substrates were then washed twice with an excess of dry toluene and acetone and cleaned by repeated sonication. The coated substrates were finally rinsed with acetone and dried at 25  $^{\circ}\text{C}$  under vacuum.

**Chromophore Layer Addition.** (i) *Film 7.* The silylated substrates were spin-coated at 2000 rpm with a 1 mM solution of **1** in  $\text{CHCl}_3$  and heated at 100–130  $^{\circ}\text{C}$  in a vacuum oven (dynamic vacuum, 15 Torr) for 15 min. The samples were next cooled to room temperature, washed twice with chloroform, immersed in acetone, and further cleaned by repeated sonication (2  $\times$  2 min). The substrates were dried under vacuum ( $10^{-3}$  Torr) at 100  $^{\circ}\text{C}$  for 5 min. (ii) *Films 8 and 9.* The silylated substrates were spin-coated at 1000 rpm with a 100 mM solution of either **2** or **3** in  $\text{MeOH}$  and heated at 120  $^{\circ}\text{C}$  in a vacuum oven (static vacuum, 15 Torr) for 20 min. The samples were cooled to room temperature, washed twice with methanol, immersed in acetone, and further cleaned by repeated sonication (2  $\times$  2 min). The substrates were finally dried under vacuum ( $10^{-3}$  Torr) at 100  $^{\circ}\text{C}$  for 5 min.

**Acknowledgment.** Research supported by the NSF MRSEC program (Grant DMR0076077 to the Northwestern Materials Research Center), by ARO/DARPA (Grant DAAD19-00-1-0368), by MIUR (Grant 2001034442\_004), and by CNR-Progetto Finalizzato Materiali Avanzati II. XRR measurements were performed at beam line X23B of the National Synchrotron Light Source, which is supported by the U.S. Department of Energy.

CM0205635